Dynamics of a water droplet over a sessile oil droplet: compound droplets satisfying a Neumann condition

R. Iqbal[1], S. Dhiman[1], A. K. Sen[1,*], A. Q. Shen[2]

[1]Department of Mechanical Engineering, Indian Institute of Technology Madras, Chennai-600036, India
[2]Micro/Bio/Nanofluidics Unit, Okinawa Institute of Science and Technology Graduate University, Okinawa, Japan

[*]Author to whom correspondence should be addressed. Email: ashis@iitm.ac.in

Abstract

We report the dynamics of compound droplets with a denser liquid (water) droplet over a less dense sessile droplet (mineral oil) that satisfies the Neumann condition. For a fixed size of an oil droplet, depending on the size of the water droplet, either it attains the axisymmetric position or tends to migrate toward the edge of the oil droplet. For a water droplet-to-oil droplet at volume ratio $V_w/V_o \geq 0.05$, stable axisymmetric configuration is achieved; for $V_w/V_o < 0.05$, migration of water droplet is observed. The stability and migration of water droplets of size above and below critical size respectively are explained using the force balance at the three phase contact line and film tension. The larger and smaller droplets that initially attain the axisymmetric position or some radial position respectively evaporate continuously and thus migrate towards the edge of the oil droplet. The radial location and migration of the water droplets of different initial size with time are studied. Experiments with water droplets on a flat oil-air interface did not show migration, which signified the role of the curved oil-air interface for droplet migration. Finally, coalescence of water droplets of size above the critical size at the axisymmetric position is demonstrated. Our compound droplet studies could be beneficial in applications involving droplet transport where contamination due to direct contact and pinning of droplets on solid surfaces is of concern. Migration and coalescence of water droplets on curved oil-air interfaces could open up new frontiers in chemical and biological applications including multiphase processing and biological interaction of cells and atmospheric chemistry.

1. Introduction

Surface tension[1] plays a crucial role in the floatation of small denser objects over surfaces of liquids[2,3]. The wettability of liquids at a solid-liquid interface is determined by the Young's contact angle[4], whereas the same at liquid-liquid interface is governed by the Neumann's triangle[5–7]. Compound droplets[8–10] or multiphase droplets that comprise two immiscible liquid droplets surrounded by another immiscible phase have found applications in many areas such as multiphase processing[11] and biological interaction of cells[11] and atmospheric chemistry[12]. Although the concept of multiphase droplets existed for almost a hundred years[13], such droplets have recently[14–16] gained considerable attention due to their potential applications in functionalized foods, pharmaceutical formulations and drug delivery vehicles[17].

The equilibrium shape of compound droplets is determined by the minimization of surface and interfacial energy of the system[18]. Investigation of the interfacial interaction of an oil droplet over water surface surrounded by air as an immiscible continuous phase has been reported[19–25]. The shape of the resulting droplets has been studied using simulations[26–28] and experiments[12]. The interfacial interaction of two immiscible liquid droplets in a third immiscible phase have been studied analytically with the help of the spreading coefficient[29]. Based on the minimization of surface and interfacial energies, mainly two possible configurations are observed[12]: droplet encapsulation and liquid lens formation, depending on the value of the spreading coefficients $S_i = \gamma_{jk} - (\gamma_{ij} + \gamma_{ik})$, where i, j and k represent the three different phases in a compound droplet, first phase, second phase and third phase (continuous phase), respectively. If the interfacial tension values are such that all the three spreading coefficients are negative, then a liquid lens of the first phase is formed over the surface of the second phase. If the spreading coefficient for the second phase is positive and that for the first and third phases are negative, then the first phase gets completely engulfed inside the second phase. Depending on the density and volume of the phases, two more configurations are also possible[12]: collar and Janus configuration. If the continuous phase is the least dense, both phases of the compound drop can be in contact with the substrate which gives rise to an axisymmetric configuration and formation of a ring or collar of first phase around the base of the sessile droplet of the second phase. If the top droplet (first phase) in a compound droplet is of larger volume such that gravity plays a role, the top droplet slides down and rests on the substrate besides the sessile droplet which gives the non-axisymmetric and non-spherical Janus configuration[7].

Most of the studies reported on the multiphase systems involving floating liquid lens are based on the floatation of less dense phase on top of the denser phase[27,30,31], which is either of planar or curved shape. A detailed description of the

formation of liquid lens with a lighter drop on top of the planar interface of a denser liquid has been studied[30]. However, when the supporting interface is curved, such as a lens on a droplet, the problem becomes challenging due to the additional complexity because of the curvature. Limited studies are available on such systems and in most cases the compound droplets are entirely surrounded by another immiscible continuous phase[32–35]. In such a case, description of the equilibrium geometrical configuration becomes relatively simple and is obtained from the Young-Laplace equation by considering the interfacial energies and drop volumes. Recently the geometric stability criterion for axisymmetric configuration[36] that is the density ratio must be smaller than the critical density ratio that depends on the surface and interfacial tensions, the drop volumes, and the contact angle, is determined in the zero bond number limit, followed by the verification by using Surface Evolver (SE) simulations and experiments. However, in these cases, the top droplet is less dense as compared to the sessile base droplet.

The flotation of a denser phase on top of less dense phase has not received much attention. The floatation of water droplet on a flat oil interface that satisfy Neumann triangle was studied experimentally[37]. It was found that the stability of the floating droplet depends on the combination of three interfacial tension values, oil density, and water droplet volume. More recently, the stability of the water droplet on flat oil interface was improved by using surfactant which changes the obtuse contact angle to acute contact angle[38]. In the above cases, the stability of the denser droplet on a less dense liquid was explained in terms of the Neumann triangle. Recently, we have reported floatation of a denser liquid drop on the flat surface of a less dense oil that do not satisfy Neumann condition ($\gamma_{ij} > \gamma_{jk} + \gamma_{ik}$) and explained the role of line tension which prevents the denser droplet from complete engulfment[39]. Here, for the first time, we report the dynamics of a denser liquid (water) droplet on the curved interface of a sessile lighter phase (mineral oil) droplet placed on a flat PDMS surface in which the Neumann condition is satisfied. For a fixed volume of sessile oil droplet, the behavior of water droplets of different volumes is investigated. Water droplets above a critical volume attain stable axisymmetric position whereas smaller droplets migrate towards the edge of the sessile droplet. The stability and migration of the water drops are explained both using force balance at the three phase contact line as well as the energy minimization perspective.
The motion of droplets on a substrate has been widely studied in which a differential curvature gradient is imposed to create a Laplace pressure gradient[40]. The velocity of a droplet is determined by balancing the force due to Laplace pressure gradient and viscous force, which in turn gives the capillary velocity of the droplet[41]. One of the major limitations of controlled motion of droplets on surfaces is due to the droplet pinning along the contact line and surface contamination[42,43]. It has been reported that external vibrations[44] or coalescence[45] can overcome droplet pinning. Here, we demonstrate transport of water droplets over droplet or curved interface of mineral oil. Since there is no direct contact between the droplet phase and the substrate, it prevents droplet pinning and eliminates contamination. The radial location of the water droplets of different initial size during migration is studied with time. Finally, coalescence of water droplets of size above the critical size at the axisymmetric position is demonstrated. In this article, we first discuss the materials and methods used for the compound droplet studies. Next, we outline the theoretical considerations for the compound droplets involving multiple interfaces. Finally, we present the experimental results and discussions.

2. Materials and methods

Deionized (DI) water was obtained from a deionization water purification system (Siemens, resistivity 18.2 MΩ.cm). Mineral oil (99% purity) was obtained from Across Organics (Thermo Fisher Scientific) and used as received. The densities of water and mineral oil are 998 kg/m^3 and 850 kg/m^3 respectively. The surface tension of DI water and mineral oil, and interfacial tension of mineral oil with DI water were measured by Du Nouy ring method using a Tensiometer (Sigma 701 Tensiometer, Sweden) and are respectively as: 72.8±0.2 mN/m, 28.8±0.2 mN/m, and 45.6±0.5 mN/m. Micro glass slides (The Science House, Chennai, India) spin coated with PDMS (Sylgard- 184, Silicone Elastomer kit, Dow Corning, USA) were used. The PDMS coated substrate is hydrophobic with DI water contact angle of 112^o and oleophilic with mineral oil contact angle of 42^o, as measured using a Goniometer (Holmarc Opto-Mechatronics Pvt. Ltd., India). The oleophilic PDMS substrate makes it easier to dispense and position the sessile mineral oil droplet to perform the compound droplet experiments. The PDMS coated glass slides were thoroughly cleaned with isopropyl alcohol (IPA) and dried with compressed nitrogen before use. Compound droplets were prepared by first dispensing fixed volume of a sessile droplet of mineral oil on the PDMS coated glass substrate, and then adding another drop of DI water on top using syringes. The volumes of the dispensed droplets were verified using a high precision microbalance (Sartorius AG, Germany). Two USB microscopes (AM7515MZT & AM7115MZT, Dinolite, Taiwan) were used for simultaneously capturing the side and top views of the compound droplets (Fig. 1a). The experiments were conducted in an air-conditioned laboratory at an ambient temperature of 22 ^{o}C with 47% relative humidity. Observation of the portion of the water droplet present inside oil droplet is challenging as the oil droplet is a portion of a spherical cap. In order to observe the water-oil interface below the three-phase contact line, we used a PDMS substrate with a cylindrical slot of diameter of the order of the base diameter of sessile oil droplets, as depicted in Fig. 1b. For better visualization of the water droplet, in some experiments a small amount of Rhodamine dye (0.5% by volume) is added to DI water. The change in the properties of DI water (i.e., density, surface tension and interfacial tension) due to addition of the dye is less than 1% so it does not influence the experimental results.

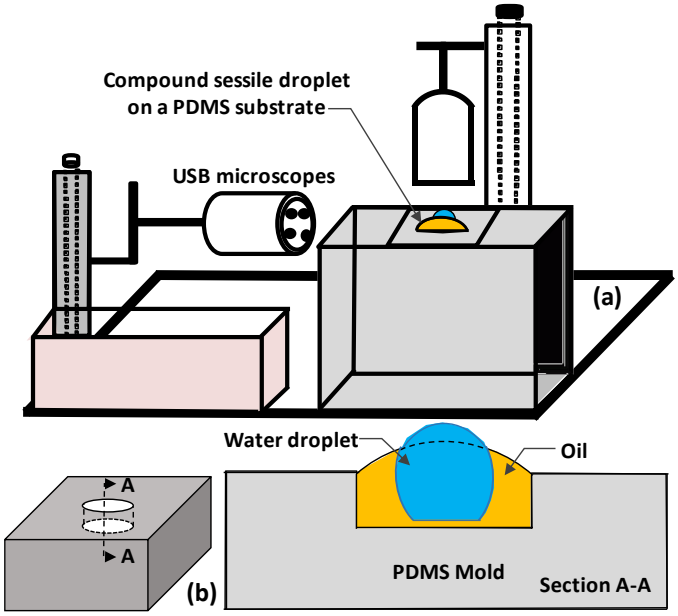

Fig. 1 (a) Schematic of the setup used in our experiments with compound droplets (b) PDMS substrate with a cylindrical slot used for observing the water-oil interface below the three-phase contact line.

3. Theoretical considerations

A schematic of a sessile compound droplet resting on a planar substrate is depicted in Fig. 2a. A small denser liquid (water, subscript w) drop is placed on top of a sessile less dense (mineral oil, subscript o) droplet both surrounded by a continuous phase (air, subscript a) so the water drop attains lens configuration. The formation of liquid lens at the interface between two immiscible liquids (i.e. water and oil) surrounded by another immiscible continuous phase (i.e. air) can be governed by Neumann triangle[5,6,30]. The Neumann triangle requires that the interfacial tensions γ_{ij} satisfy the triangle inequality $\gamma_{ij} < \gamma_{jk} + \gamma_{ki}$ for all cyclic permutation of the indices $(i,j,k) = (w,o,a)$, which is satisfied for the water-mineral oil-air combinations.

In order to verify for the effect of gravity on the behaviour of the compund droplet, we consider the interfacial tension γ_{ij} of the different interfaces and the corresponding Capillary length $\lambda_{ij} = \sqrt{\gamma_{ij}/\Delta\rho_{ij}g}$, where $\Delta\rho_{ij}$ is the density difference between the phases i and j, and g is the acceleration due to gravity. For the fluid system considered here, the capillary length $\lambda_{ij} \geq 5.6$ mm and the typical length scale L of the water drops we consider is $L \cong 0.78$ mm, which gives the corresponding Bond number $Bo \equiv \left(L/\lambda_{ij}\right)^2 \cong 0.019 \ll 1.0$. This indicates that the effect of gravity on the behaviour of the compound droplet can be neglected.

In the case of liquid lenses, at three phase contact line, line tension τ can be important[30]. However, the effect of line tension on the equilibrium behavior of a system diminishes when the contact radius r_c at the three phase contact line is large. As reported in the literature[31,46], the values of line tension are in the range of 10^{-9} to 10^{-12} J/m. In our experiments, the radius at the three phase contact line $r_c \sim 10^{-3}$ m, and the values of interfacial tensions $\gamma_{ij} \sim 10^{-3}$ N/m. Since $(\tau/r_c) \ll \gamma_{ij}$, the influence of the line tension on the equilibrium behavior of the compound droplet can also be neglected.

In the compound droplet (Fig. 2a), by considering Young-Laplace pressure jump across the water-oil interface[12], we obtain

$$\frac{\gamma_{wa}}{r_{wa}} = \frac{\gamma_{oa}}{r_{oa}} + \frac{\gamma_{wo}}{r_{wo}}. \tag{1}$$

The geometry of the triangles in Fig. 2a gives

$$r_{wo}sin\theta_{wo} = r_{wa}sin\theta_{wa} = r_{oa}sin\theta_{oa} = r_{c.} \tag{2}$$

Considering conservation of volumes of the water and oil droplets of initial radius R_w and R_o , respectively, we obtain

$$R_w^3 = (r_{wa}^3/4)[2 + 3cos\theta_{wa} - cos^3\theta_{wa} + \xi_{wo}] \text{ and}$$

$$R_o^3 = (r_{oa}^3/4)[2 + 3cos\theta_{oa} - cos^3\theta_{oa} - \xi_{wo}],$$

where $\xi_{wo} = r_{wo}^3(2 - 3cos\theta_{wo} + cos^3\theta_{wa})$, represents the volume of the water droplet inside the oil phase. (3)

If we balance interfacial tension forces along the horizontal direction, we get

$$\gamma_{wa}cos\theta_{wa} + \gamma_{oa}cos\theta_{oa} = \gamma_{wo}cos\theta_{wo} \quad (4)$$

If we introduce the following non-dimensional parameters: $K_w = \gamma_{wa}/\gamma_{wo}$, $K_o = \gamma_{oa}/\gamma_{wo}$ and $C_a = r_{wa}/r_{oa}$, eqns. 1 and 2 can be expressed as

$$r_{wo} = r_{wa}/(K_w - C_aK_o) \quad (5)$$

$$sin\theta_{wo} = sin\theta_{wa}(K_w - C_aK_o) \text{ and}$$

$$sin\theta_{oa} = C_asin\theta_{wa} \quad (6)$$

Upon substitution of eqns. 5 and 6 in eqn. 4, we get

$$sin^2\theta_{wa} = [4K_w^2K_o^2 - (1 - K_w^2 - K_o^3)^2]/4\Gamma \text{ ,} \quad (7)$$

where $\Gamma = K_wK_o[K_wK_o(C_a^2 + 1) - C_a(K_w^2 + K_o^2 - 1)]$.

By combining eqn. 7 with eqn.6, we obtain

$$cos\theta_{wa} = [2K_wK_oC_a - (K_w^2 + K_o^2 - 1)]/2\Gamma^{1/2},$$

$$cos\theta_{wo} = [C_aK_0(K_w^2 - K_o^2 + 1) - K_w(K_w^2 - K_o^2 - 1)]/2\Gamma^{1/2} \text{ and}$$

$$cos\theta_{oa} = [2K_wK_o - C_a(K_w^2 + K_o^2 - 1)]/2\Gamma^{1/2} \quad (8)$$

From geometry, the contact angles δ, ϕ and ψ at the three phase contact line (Fig. 2b) and the angles θ_{wa}, θ_{oa} and θ_{wo} are related as follows:

$$\delta = \theta_{wo} + \pi - \theta_{wa}, \phi = \theta_{wa} + \theta_{oa}, \psi = \pi - \theta_{wo} - \theta_{oa} \quad (9)$$

Upon substitution of eqn. 8 in eqn. 9, we express the three phase contact angles δ, ϕ and ψ in terms of the interfacial properties. The contact angle δ is obtained as

$$cos\delta = cos(\alpha + \beta) = (\gamma_{oa}^2 - \gamma_{wa}^2 - \gamma_{wo}^2)/2\gamma_{wa}\gamma_{wo} \quad (10)$$

Similarly, $cos\phi = (\gamma_{wo}^2 - \gamma_{oa}^2 - \gamma_{wa}^2)/2\gamma_{oa}\gamma_{wa}$ and $cos\,\psi = (\gamma_{wa}^2 - \gamma_{wo}^2 - \gamma_{oa}^2)/2\gamma_{wo}\gamma_{oa}$.

If we balance the components of the interfacial tensions in the directions along parallel and normal to the oil-air interface at the three-phase contact line, we would acquire two equations that are equivalent to the Neumann triangle condition, as follows

$$\gamma_{wa}cos(\beta - \omega) + \gamma_{wo}cos(\alpha + \omega) = \gamma_{oa} \text{ and} \quad (11)$$

$$\gamma_{wa}sin\,(\beta - \omega) - \gamma_{wo}sin(\alpha + \omega) = 0$$

The above two equations can be solved to give

$$cos(\alpha + \omega) = [1 + (\gamma_{wo}/\gamma_{oa})^2 - (\gamma_{wa}/\gamma_{oa})^2]/2(\gamma_{wo}/\gamma_{oa}) \text{ and}$$

$$cos(\beta - \omega) = [1 + (\gamma_{wa}/\gamma_{oa})^2 - (\gamma_{wo}/\gamma_{oa})^2]/2(\gamma_{wa}/\gamma_{oa}) \text{ .} \quad (12)$$

By solving eqns. 10 and 12, we can obtain the values of α, β and ω which can be used for calculating the net vertical and horizontal forces at the three phase contact line.

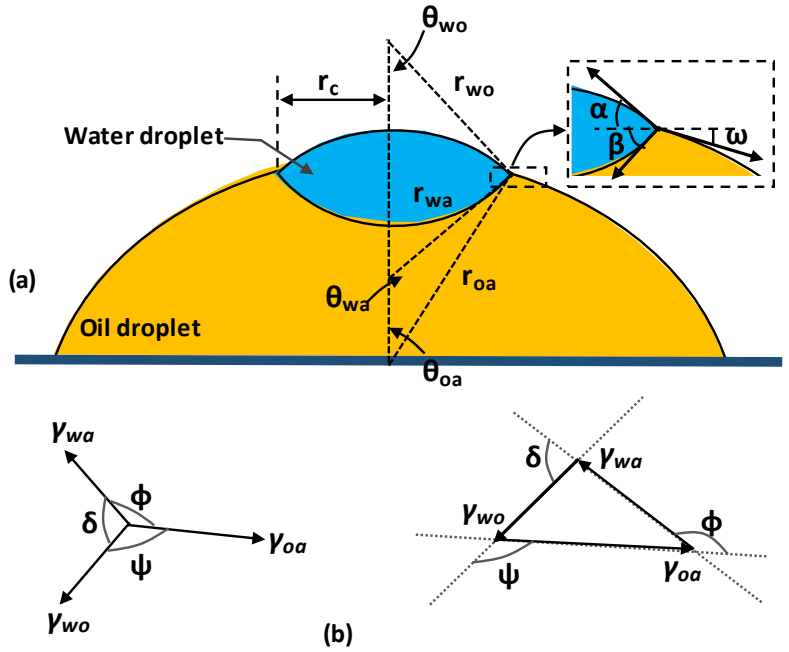

Fig. 2 (a) Schematic of a compound droplet, with water droplet on a sessile oil droplet, resting on a planar substrate and surrounded by air as the continuous phase; (b) Equilibrium interfacial tensions and the corresponding closed Neumann triangle.

4. Results and discussion

4.1 Behavior of compound droplets: the critical size

First, we performed experiments to observe the behavior of compound droplets by varying the volumes of the oil and water droplets. Fig. 3a shows experimental images of DI water droplets of volume V_w = 0.25 and 2.0 µl over sessile mineral oil droplets of fixed volume V_o =15 µl resting on PDMS surface. In both cases, the water droplets were dispensed precisely at the top axisymmetric location of the mineral oil droplets. It is observed that the larger DI water droplet of size V_w = 2.0 µl attains stable axisymmetric configuration while the smaller DI water droplet of size V_w = 0.25 µl migrates toward the edge of the sessile oil droplet. This non-intuitive behavior of compound droplets were investigated further by varying the size of the oil and water droplets systematically. The volume of the sessile oil droplet was varied in the range of V_o =5.0 to 15.0 µl (with increment of 2.5 µl) and for each volume of the oil droplet, DI water droplets of volume in the range of V_w =0.25 to 1.5 µl (with increment of 0.25 µl) were used. Fig. 3b shows the experimental data for the migrating and non-migrating (stable) compound droplets for different combinations of volumes of oil and water droplets. For a given volume of sessile oil droplet, there is a critical volume of water droplet V_c above which the compound droplet remains stable at the axisymmetric position and below which outward migration of DI water droplet is observed. Interestingly, the critical volume V_c linearly increases with the increasing volume of the sessile oil droplet V_o which gives V_c = 0.05 V_0 (Fig. 4). The stability of droplets of size above the critical volume and migration of droplets of size below the critical volume are explained in section 4.1 and 4.2, respectively.

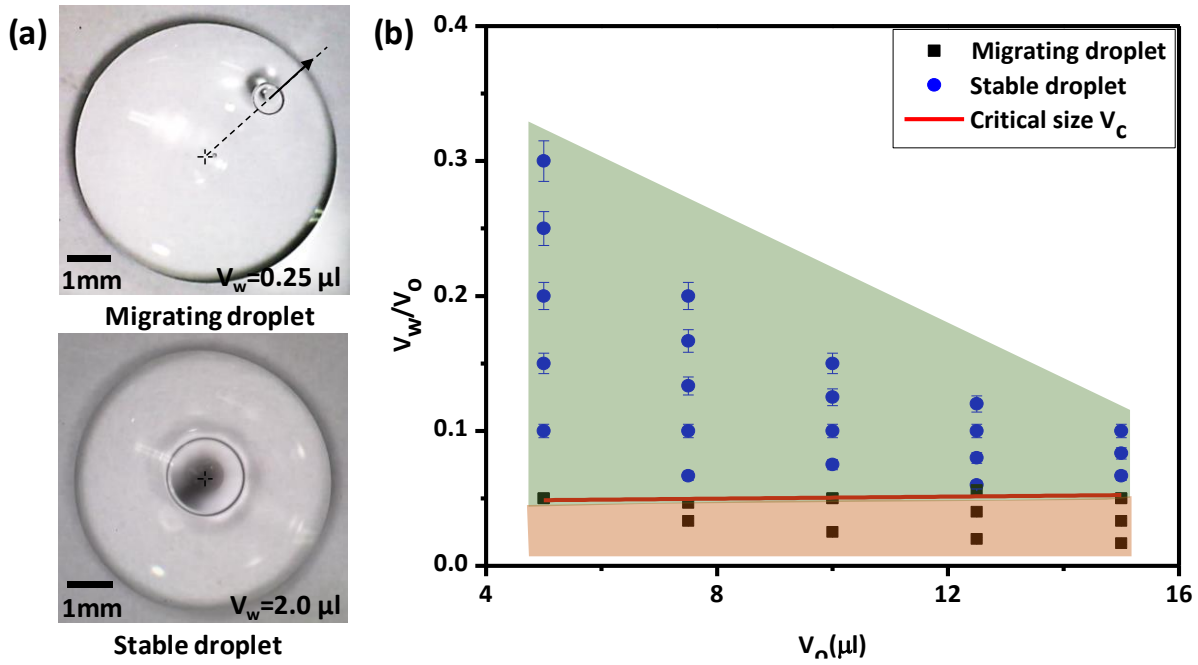

Fig. 3 (a) Behavior of DI water droplets of volume V_w = 0.25 and 2.0 µl over sessile oil droplets of fixed volumes V_o =15 µl resting on PDMS surface (b) Experimental data for the migrating and stable compound droplets for different combinations of volumes of oil V_o and water V_w droplets.

4.2 Water droplets larger than the critical size: migration and temporary equilibrium

Next, we performed experiments with water droplets of volumes larger than the critical size and observed the migration behavior. Fig. 4a shows the migration behavior of a larger water droplet of volume 2.0 µl dispensed off-centered (r = 0.47 mm) on a sessile mineral oil droplet of volume 15 µl. In less than 6.0 s, the water droplet migrates toward the center of the oil droplet and attains stable axisymmetric configuration (temporarily). The migration of droplets larger than the critical size toward the axisymmetric position can be explained with the help of Fig. 4b. A water droplet of larger than critical size contacts the substrate at a location where it is dispensed and is deformed asymmetrically with varying radii of curvature which results in a differential Laplace pressure $\Delta p = \gamma_{wo}(1/R_o - 1/R_i)$, where R_o and R_i are the radius of curvature of the outer and inner sides of the water-oil interface. The differential Laplace pressure propels the droplet toward the axisymmetric position for the minimization of surface energy. In order to view the water-oil interface below the three phase contact line, we performed experiments with a PDMS substrate containing a cylindrical slot (Fig. 1b) of diameter comparable to that of the base diameter of the 20 µl droplet. A water droplet of volume 3.0 µl was dispensed at an off-centered position on the curved mineral oil interface and the images are presented in Fig. 4c (also in Video S1 in the Supporting Information). Due to the differential Laplace pressure resulting from this difference between the radii of curvature, the droplet migrates toward the center and attains axisymmetric configuration at t =15 s.

The water droplets of volume (2 µl) above the critical size remain at the axisymmetric configuration in a stable manner for some time (~50 min). The interfacial energy of water with PDMS is higher than the sum of the interfacial energies of mineral oil with PDMS and water i.e. $\gamma_{ws} > \gamma_{os} + \gamma_{wo}$, where γ_{os} and γ_{ws} are the interfacial energies of mineral oil and water with PDMS substrate. Thus there will always be a thin film of oil between the water droplet and PDMS substrate (Fig. 4b). The interfacial tensions involving the solid surface γ_{ws} and γ_{os} are difficult to measure. However, $(\gamma_{ws} - \gamma_{os})$ can be determined by measuring the contact angles of water and oil on the solid surface and using Young's law as follows[47]: $\Delta\gamma = (\gamma_{ws} - \gamma_{os}) = \gamma_{oa}cos\theta_o - \gamma_{wa}cos\theta_w - \gamma_{wo}$, where θ_o and θ_w are the contact angles of mineral oil and water with PDMS, respectively. In the present case, the measured contact angles of the water and mineral oil with PDMS respectively are θ_w =112°, θ_o =42°. By substituting the interfacial properties (given in section 2), we find that $\Delta\gamma > 0$, thus there is always a thin layer of oil between the water droplet and PDMS substrate, which prevents pinning of water droplets[38]. By treating the PDMS surface with oxygen plasma for 1.0 min, the contact angles are measured to be θ_w =5°, θ_o =34° and we find that $\Delta\gamma < 0$. In this case, the thin layer of oil is not formed and instead the water and oil droplets attain the Janus configuration[7].

The equilibrium of the water droplet (temporary) at the axisymmetric configuration can be explained by the balance of forces acting on the water droplet. In addition to the interfacial tensions, the film tension γ_F also contributes towards the

balance of forces (Fig. 4b). The film tension[48–51] γ_F is due to the contributions of both the oil-air γ_{oa} and oil-water γ_{wo} interfacial tensions. For larger droplets, the balance of vertical forces acting on the water droplet can be expressed as

$$F_{uv} = 2\pi r_c(\gamma_{wo} sin\beta + \gamma_{oa} sin\omega - \gamma_{wa} sin\alpha) - 2\pi R_F \gamma_F sin\theta_F \quad (13)$$

where R_F is the contact radius of water droplet with the thin film of oil on the substrate and θ_F is the contact angle of the water droplet on the oil film. For the case of 3.0 µl droplet at the axisymmetric configuration, by substituting the contact radius r_c, interfacial properties γ_{wo}, γ_{oa} and γ_{wa} (from section 2), angles α, β and ω at the three phase contact line, contact radius R_F and contact angle θ_F (from Surface Evolver[43] simulations), we find that $F_{uv} \approx 0$. Similarly, due to the axisymmetric nature of the three phase contact line, the net horizontal force acting on the water droplet $F_{uh} \approx 0$. Since both the horizontal and vertical forces acting on the droplet vanish, the larger droplets remain stable at this position. However, the larger stable water droplets (initial volume V_{wi} =2 µl) at the axisymmetric position evaporate continuously with time t and become smaller in size over time and tend to lose contact with the substrate (after a duration of 50 min). The variation of the instantaneous volume of water droplet of initial size 2µl with time is shown in Fig. 5. The results show that the droplet volume varies with time as $V(t) = 2.5\, exp(-t/70) - 0.5$. When the droplets become smaller in size (0.75 µl, at t=50 min), the film tension becomes obsolete, and the net force acting on these droplets becomes non-zero and the droplets start to migrate radially outward, which is discussed further in detail.

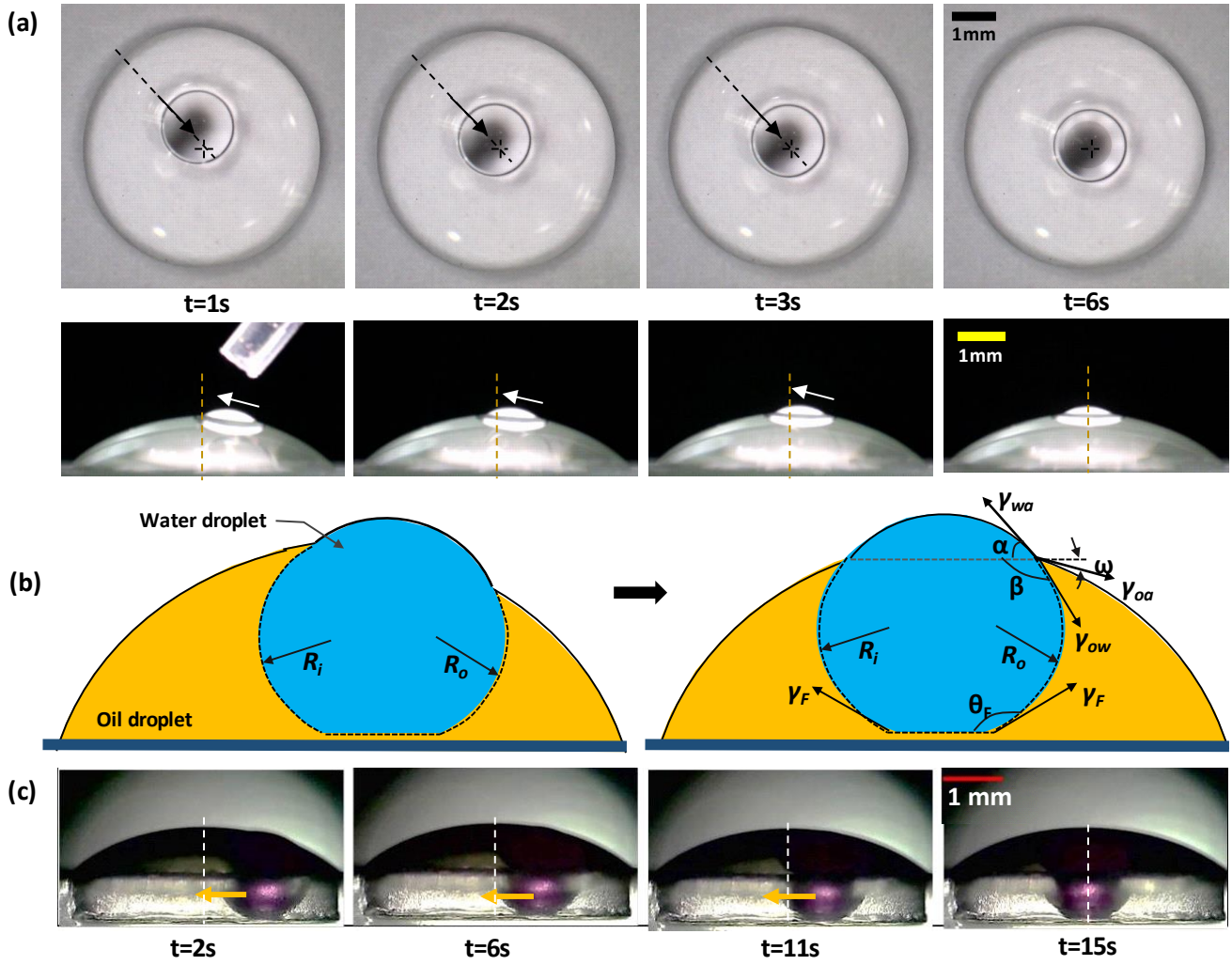

Fig. 4 (a) Migration of 2 µl (stable) water droplet over 15 µl mineral oil droplet; (b) Schematic of compound droplets of volume above critical size; (c) Migration of 3 µl of water droplet (with 0.5% Rhodamine, shown in purple) over 20 µl of mineral oil droplet in a cylindrical slot

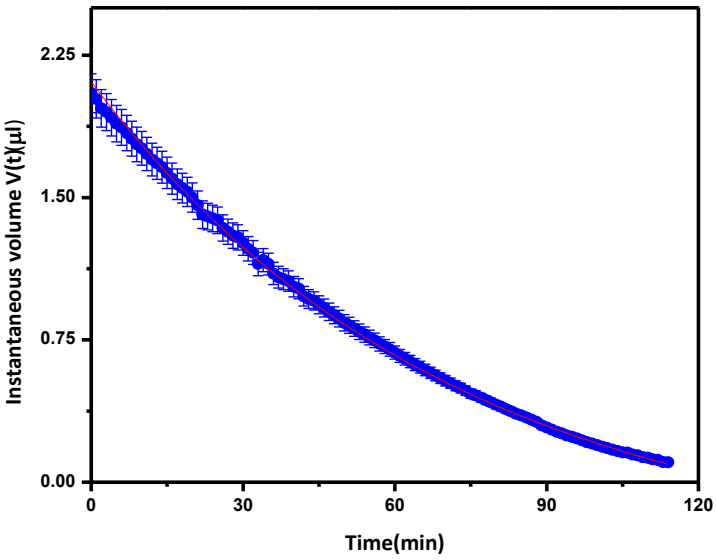

Fig. 5 The instantaneous volume of water droplet $V_w(t)$ varies with time t, with an initial volume of 2 µl.

4.3 Water droplets smaller than the critical size: migration and temporary equilibrium

The migration behavior of water droplets of volumes smaller than the critical size (shown in Fig. 3a) can be explained by the balance of forces acting on the droplets. If a smaller water droplet is dispensed at the axisymmetric position or a larger stable water droplet already present at this position evaporates and becomes smaller, the net vertical component of the forces acting on the droplet is obtained from the force balance at the three phase contact line and can be expressed as

$$F_{uv} = 2\pi r_c(\gamma_{wo} sin\beta + \gamma_{oa} sin\omega - \gamma_{wa} sin\alpha). \quad (14)$$

For the compound droplets under study, by substituting the interfacial tensions in eqns. 10 and 12, the values of the three phase contact angles α, β and ω are determined. By using the three phase contact angles in eqn. 14, in the case of droplets of volume smaller than the critical size, we find that there is an unbalanced downward force acting on the droplets, i.e. $F_{uv} \neq 0$. Similarly, the net horizontal force acting on the water droplet can be expressed as

$$F_{uh} = \oint(\gamma_{oa} cos\omega - \gamma_{wo} cos\beta - \gamma_{wa} cos\alpha)\, dS, \quad (15)$$

where S denotes the spatial coordinate along the three phase contact line. When a water droplet smaller than the critical size is located at the centre of the oil droplet, the horizontal components of the interfacial tensions will be axisymmetric thus the net horizontal force F_{uh} acting on the water droplet becomes zero. However, spatial inhomogeneity in the interfacial properties or external perturbations causing a small shift of the water droplet from the axisymmetric position, could lead to $F_{uh} \neq 0$, although very small. The non-zero force acting on a water droplet in the vertical direction F_{uv} given by eqn. 14 along with a small component of the force in horizontal direction F_{uh} (due to spatial inhomogeneity) given by eqn. 15 result in the migration of droplets of size smaller than the critical size. The migration of such smaller droplets (of size below critical size) can also be explained by finding out the net force which is the difference between the weight and buoyancy forces acting on the droplets as $F_{net} = (\rho_w g V_w - \rho_o g V_{ow})$, where ρ_w and V_w are the density and volume of water droplet, respectively and ρ_o and V_{ow} are the density of oil and volume of the water droplet inside the oil interface, respectively. The net force acting on the water droplet F_{net} is non-zero which leads to droplet migration.

Fig. 6a show the top views of a compound droplet at various time instants with sessile mineral oil droplet of volume 15 µL and water droplet of volume 0.25 µl. Since the volume of the water droplet is smaller than the critical size, due to the unbalanced force given by eqn. 14, the water droplet migrates toward the edge of the sessile oil droplet. In order to view the water-oil interface below the three phase contact line, we used a PDMS substrate with a cylindrical slot illustrated in Fig. 1 and the images for 1.0 µl of water droplet are presented in Fig. 6b (also in Video S2 in the Supporting Information). As observed, for a fixed size of oil droplet, when water droplets of size smaller than critical size are dispensed on the sessile oil droplet, these water droplets do not contact the substrate and migrate radially outward until the droplets contact the substrate. The variation of the locations of the migrating droplets of different initial size with time is depicted in Fig. 7. As expected, the smaller droplets migrate longer distance before coming in contact with the substrate and attain temporary equilibrium. Here we report that our experimental data reinstates what was expected physically. As observed, the droplets of volume 0.25 µl, 0.50 µl and 0.75 µl instantaneously travel radial distances of 1.93 mm, 1.37 mm and 0.89

mm, respectively, before attaining temporary equilibrium configuration. At these temporary equilibrium locations, the droplets contact with the substrate and the net force acting on the droplets become zero. The water droplets continuously evaporate and as the droplets lose contact with the substrate they tend to migrate toward the edge of the droplet. However, in the experiments some hysteresis was observed even though the droplets were losing contact with the substrate, the droplets did not migrate immediately. The possible reason for the hysteresis can be explained as follows: a droplet of size larger than the critical size, initially located at the center in a stable manner, evaporates and tends to lose contact with the substrate. However, the droplet may not loose contact with the substrate uniformly at its bottom due to surface inhomogeneity thus giving rise to a range of contact angles for small changes in the droplet volume. Also, during evaporation, a water droplet is pulled downward into the oil droplet due to the unbalanced downward force but as the radius at the three phase contact line decreases, the line tension becomes significant, which prevents the droplet from moving downward. The effect of the line tension coupled with the non-uniform contact angle at the bottom of the droplet may be attributed to the observed hysteresis. Finally, when the droplet becomes very small, it is suddenly lifted up and migrates radially outward.

The smaller droplets evaporate much faster as compared to the larger droplets due to its larger surface area to volume ratio and the hysteresis is lower. Fig. 7 shows that the smaller droplets remain at the equilibrium position for a shorter duration of time. The droplets of size 0.25 µl, 0.50 µl and 0.75 µl remain in equilibrium for a duration of 3 min, 10 min and 17 min, respectively. As discussed, at the temporary equilibrium positions, as the water droplets evaporate and become smaller, these droplets no longer remain in contact with the substrate. When the droplets become smaller, the net force acting on these droplets become non-zero and the droplets continue to migrate radially outward. After the temporary equilibrium, the droplets migrate continuously toward the edge of the droplet due to continuous evaporation. As observed from Fig. 7, irrespective of the initial size, all the droplets finally arrive at the edge of the sessile oil droplet (i.e. r=2.84 mm). The time instant at which the different droplets arrive at the edge of the sessile oil droplet is proportional to their initial volume. The droplets of size 0.25 µl, 0.50 µl and 0.75 µl arrive at the edge of the sessile oil droplet at $t =$ 25, 36 and 48 min, respectively.

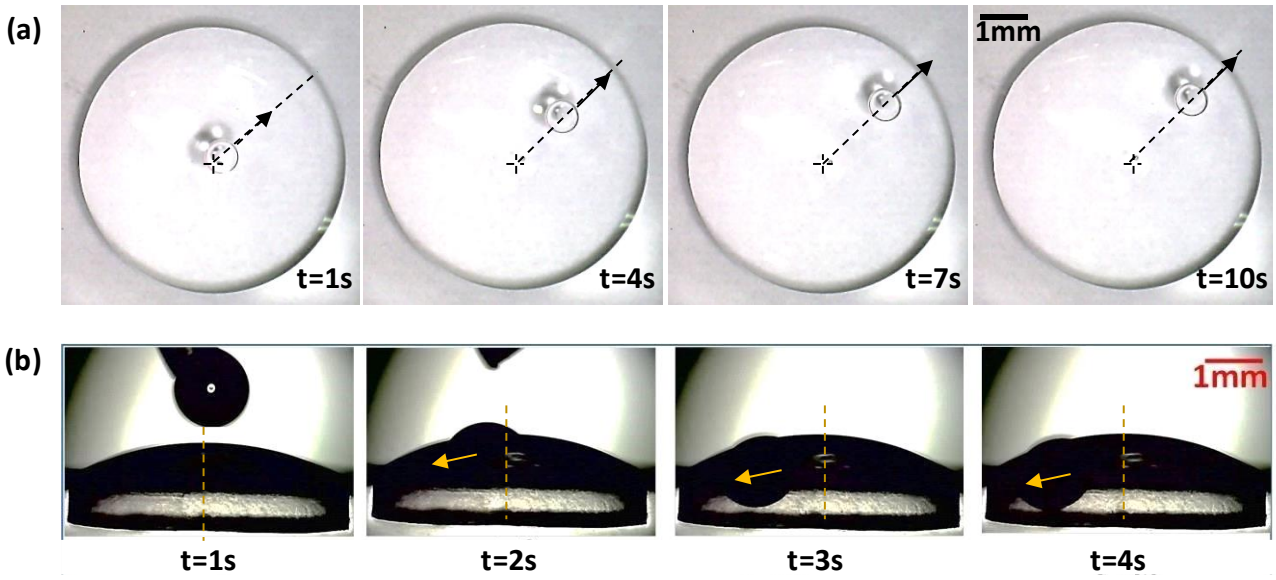

Fig. 6 (a) Top views of migrating compound droplet at different time instants, 0.25 µl water droplet on top of 15µl mineral oil droplet (b) Migration of 1.0 µl water droplet on top of 15 µl mineral oil droplet in a cylindrical slot.

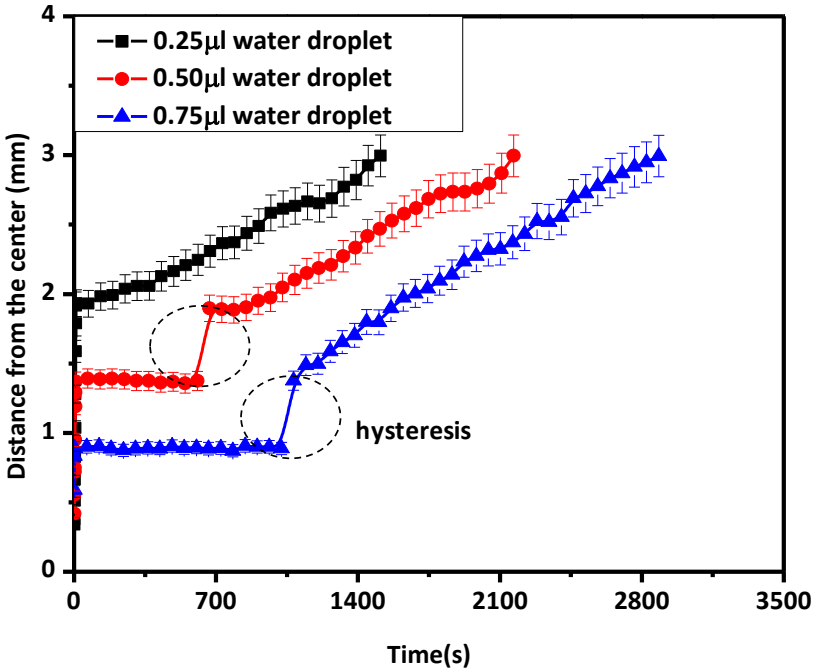

Fig. 7 The variation of the locations of the migrating droplets with respect to time, with different initial volumes.

4.4 Stability and Energy minimization of water droplet:

We have reported the dynamics of the water droplet of above and below critical sizes over a sessile curved mineral oil interface. The stability and the migration of such droplets are discussed using force balance at the three phase contact line. Here in this section we have reported the energy associated with different sizes of water droplet (both above and below critical) and the stability and energy minimization of the water droplet. The detailed calculation is out of the scope of this work. We have just reported a simplified scaling analysis to support the energy minimization for both the cases. (See the details in the supporting information)

As for the droplets of below critical sizes, the free energy ($G \sim \Sigma(\gamma_i A_i)$ is a function of radius of three phase contact line (r_c) only [As the angles (α, β, ω) associated with three surface and interfacial tensions with respect to the three phase contact line are function of surface and interfacial tensions only reported by Torza et al.[29]] (Refer supplementary information). So for the droplets of below critical size, the free energy will increase with proportion to the square of the size of the droplet ($G \sim r_c^2$).So droplets of below critical size, dispensed at the axisymmetric position, will always migrate radially outward to minimize the energy by coming in contact with the substrate. But once the droplet touches the substrate, the free energy ($G \sim \Sigma(\gamma^*_i A^*_i)$ associated with the droplet, is a function of three phase contact radius as well as the angles associated with the three phase contact line, the contact radius of water droplet with the thin film of oil on the substrate (R_F), the contact angle of the water droplet on the oil film (θ_F) and the film tension. Here the free energy of the droplet although will increase with the increase in radius (r_c) but decreases with the increase in the angles mentioned. (Please see the Supporting Information for the Scaling Analysis). So there will be a critical size of the water droplet for the particular volume of oil droplet, above which the energy of the droplet minimizes by coming in contact with the substrate and the droplet becomes stable (temporarily) with that energy minimized state. Here in Figure (8) a plot has been shown where free energy of the water droplet with different sizes are studied by using surface evolver simulation. We have simulated a15 µl mineral oil droplet with different sizes of water droplet. Once the droplet touches the substrate, the angles (α, β, ω), three phase contact radius (r_c), and the contact radius (R_F) as well as the angle (θ_F) associated with that water droplet are measured and used to calculate the energy of the droplet. It is clearly depicted from the plot that for the droplets of below critical size, as the size (or volume) increases, the energy will increase in proportion to the square of the contact radius, and as a result it migrates radially outward to minimize its energy, and once the droplet touches the substrate, due to the film tension the energy of the droplet is minimized and the droplet becomes stable.

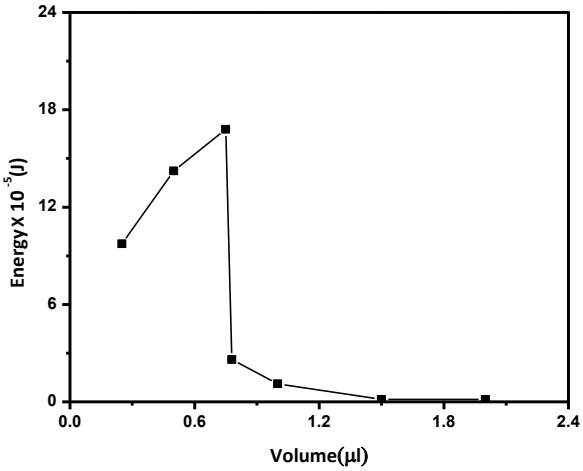

Fig. 8 The free energy associated with the water droplets of above and below critical size.

4.5 Behavior of water droplets on flat and curved oil-air interfaces

We have performed experiments by dispensing water droplets on flat and curved interfaces of mineral oil to demonstrate the role of the shape of the oil-air interface in droplet migration. Fig. 9a (also Video S3 in Supporting Information) shows the behavior of 2.0 µL water droplet on flat oil-air interface created using PDMS substrate with a cylindrical slot of base diameter 4.8 mm. In the case of the flat oil-air interface, the water droplet is initially in contact with the substrate, but evaporates and completely detaches from the PDMS substrate at $t = 90$ min. However, the water droplet does not migrate and remains stable at the same location. The water droplet continues to remain at the same location and completely evaporates at $t = 114$ min. The behavior of a 7 µl water droplet on a curved oil interface, created by dispensing oil inside a cylindrical slot, is depicted in Fig. 9b (also in Video S4 in Supporting Information).In the case of curved oil-air interface, since the since the droplet volume (i.e., 7.0 µl) is higher than the critical size, it instantaneously migrates toward the axisymmetric position, as illustrated in section 4.2. Due to evaporation, at t=124 min, the droplet becomes smaller than the critical size, thus instantaneously moves radially outward and attain a temporary equilibrium position (at $t = 125$ min), as discussed earlier. Due to continuous evaporation, the droplet becomes smaller and continuously migrates toward the edge of the oil droplet (arrives the edge at $t = 147$ min) to minimize energy. From above, it is clear that water droplets migrate on curved oil-air interfaces but remain stable on flat oil-air interfaces.

In the case of flat oil-air interface, translational symmetry exists along the oil-air interface, i.e., the surface energy remains the same for any position of the water droplet on the flat oil interface. On the other hand, in the case of a curved oil-air interface, the symmetry is lost and more complex geometry arises, which facilitates the migration of the droplets for the minimization of energy. Migration of aqueous droplets on curved oil-air interfaces as described above could be beneficial in applications involving droplet transport where contamination due to direct contact and pinning of droplets on solid surfaces is of concern. From Fig. 7, we observe that irrespective of the initial droplet size, once the temporary equilibrium is lost, all the droplets achieve a constant linear velocity ~0.8 µm/s radially outward (i.e. the slope of the curves in Fig. 7). Since the Reynolds number associated with the movement of the water droplet is very small i.e.$Re << 1$, the flow is in the "creeping flow" regime in which viscous drag becomes important. The characteristic size of the water droplet is smaller than the Capillary length scale, so it takes a shape of a spherical cap in the oil phase. The viscous drag force acting on the water droplet can be expressed as$F_d \sim \alpha \mu R V$, where μ is the viscosity of the oil, R is the radius of the water droplet and α is geometric constant, which depends on the shape of the water droplet. In this case, the net interfacial force (given by eqn. 15 and 16) is balanced by this viscous drag to give rise to a near universal velocity. Although the viscosity[52–56] does have some effect on the dynamics of the evaporation which is beyond the scope of this work. However, in the present manuscript, the objective of reporting evaporation of the water droplet in is to emphasize the role of the curved interface of the base mineral oil droplet on the migration behaviour of the water droplet. The results showed that, for flat oil interface, migration of water droplet is not observed due to the translational symmetry, even though the water droplet loses its contact from the substrate. But, for the curved oil interface, the size based migration of water droplets is observed.

Next, we study the behavior of two droplets of size 2.5 µl each that are above the critical size, on flat and curved oil-air interfaces, as shown in Fig. 10a and b, respectively. On a flat oil-air interface, the two droplets remain in their original position where they are initially dispensed. However, on a curved oil-air interface, the two droplets migrate toward the axisymmetric position and get coalesced. Fig. 10b shows the top and side views of coalescence of water droplets of volume 2.5 µl on a sessile oil droplet of volume 20 µl. The two droplets dispensed initially at $t = 0$ with an offset of 2.18 mm from the center migrate and coalesced at $t = 5.0$ s.

Once the two water droplets of size above the critical size are dispensed on the oil droplet, the water droplets migrate (due to the differential Laplace pressure) toward the axisymmetric position to minimize their energy, as explained in section 4.2. As the droplets migrate radially inward and approach each other, the drainage of thin film of oil present between the two approaching water drops take place[57]. The viscous flow of the oil enclosed in the progressively thinning film produces a dissipative force that hinders the coalescence. In addition to the Laplace pressure gradient, when the two water droplets are in close proximity, the molecular attractive energy estimated by Lennard-Jones potential becomes effective. This attractive potential constitutes the driving force for the ultimate deformation of the drops and the final drainage of the interposed film and the coalescence of droplets. Recently, non-coalescence of water droplets on an oil infused super hydrophobic surface due to the spontaneous formation of microscopic oil film between the droplets has been reported[58]. The duration of non-coalescence of water droplets was found to be one to three orders of magnitude longer as compared to submerged water droplets in an oil bath when brought in contact. Here, due to the curved interface of the base oil droplet, the driving Laplace pressure gradient helps in the coalescence process and the coalescence time in the present case was measured to be <5 s, which is three orders of magnitude smaller than that reported in literature[58]. The non-coalescence of water droplets on a flat interface and smaller coalescence time in the present case clearly bring out the advantages of coalescence of droplets on a curved interface of an immiscible liquid.

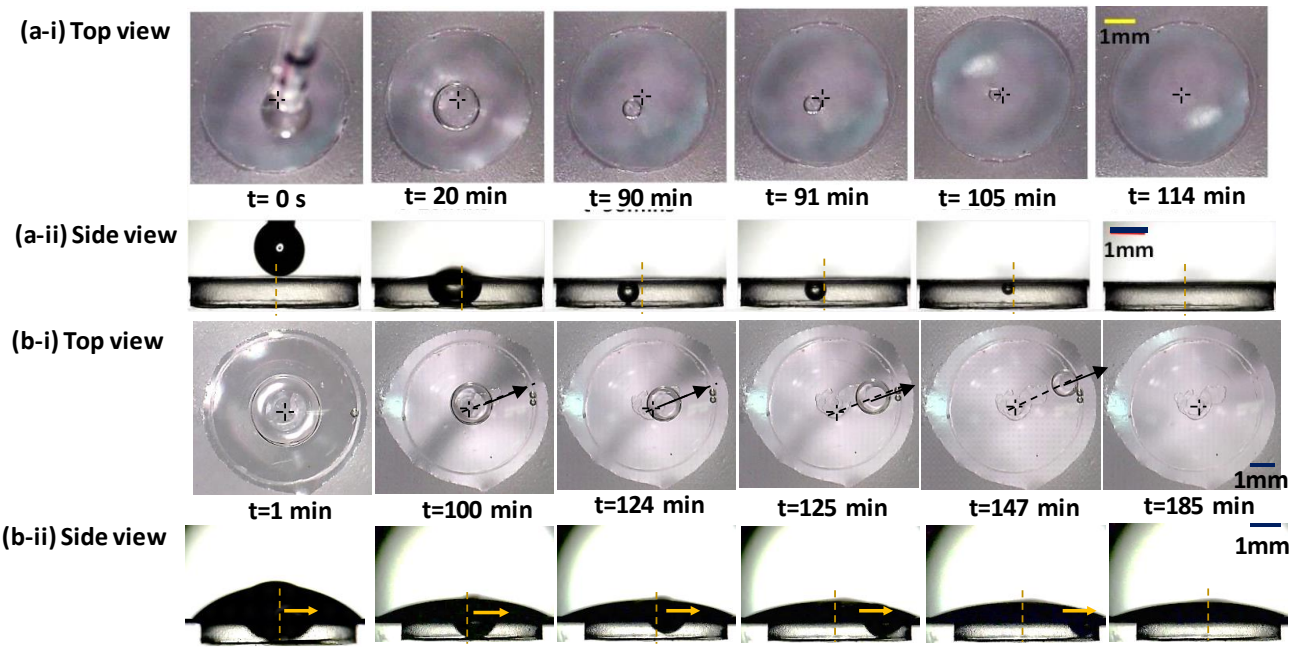

Fig. 9 (a) Behavior of 2.0 µL water droplet on flat oil interface created using PDMS substrate with a cylindrical slot of base diameter 4.8 mm; (b) The behavior of a 7 µl water droplet on a curved oil interface, created by dispensing oil inside a cylindrical slot.

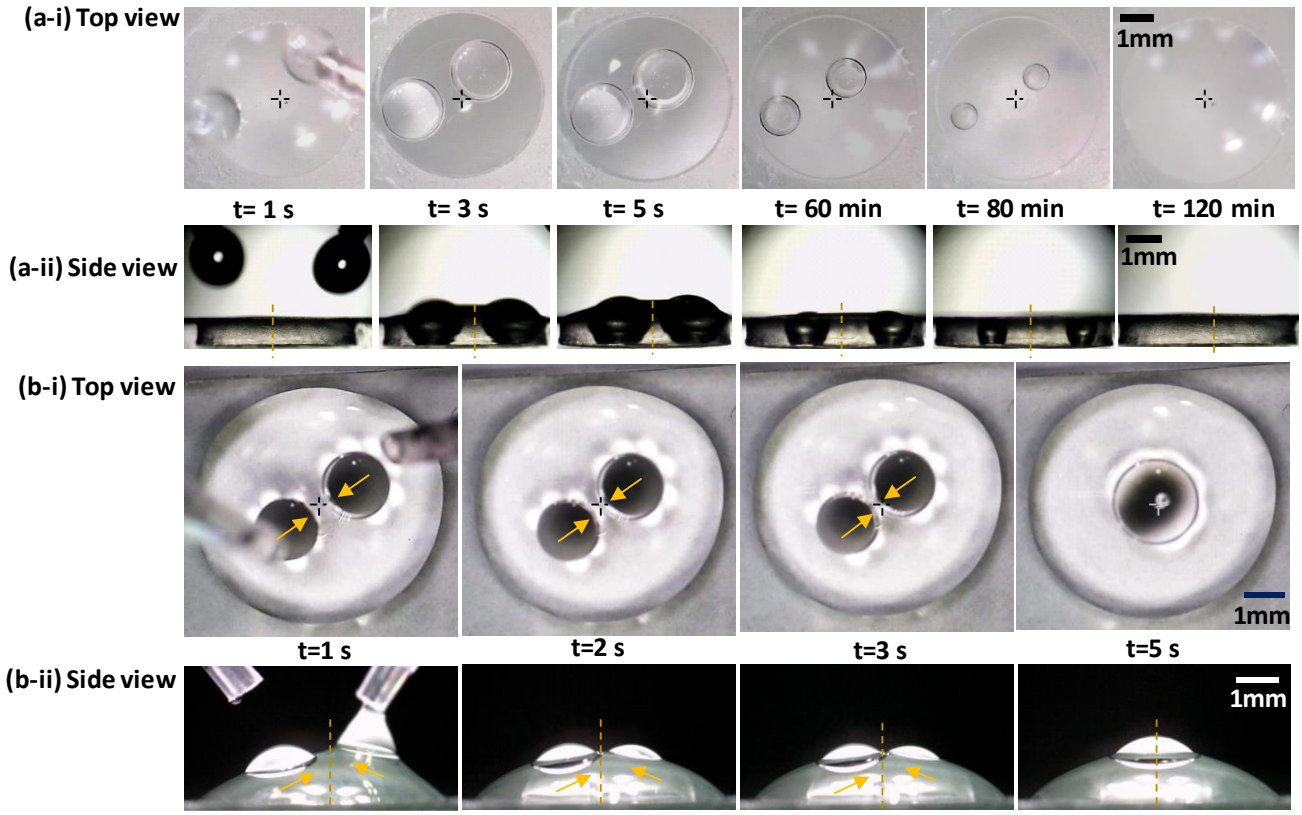

Fig. 10 (a) Behavior of two 3.0 µl water droplets floating on flat mineral oil-air interface, (i) top and (ii) side views are shown; (b) Coalescence of two 2.5 µl water droplets on top of 20 µl sessile mineral oil droplet, (i) top and (ii) side views are shown.

5. Conclusions

The dynamics of a compound droplet comprising a denser liquid (DI water) droplet on a sessile less dense liquid (mineral oil) droplet that satisfy the Neumann's triangle was studied. For a fixed volume of the sessile mineral oil droplet, depending on the volume of the water droplet, the water droplet either attains stable axisymmetric configuration or migrate toward the edge of the sessile oil droplet. Stable axisymmetric configuration was observed for a water-to-oil droplet volume ratio $V_w/V_o \geq 0.05$ and radially outward migration of water droplet was observed for $V_w/V_o < 0.05$. It was observed that larger droplets dispensed off-centered have asymmetric radius of curvature of the water-oil interface on the inner and outer sides, which give rise to Laplace pressure gradient that propels the droplets toward the axisymmetric position. The stability of the droplets larger than the critical size at the axisymmetric position was explained in terms of force balance involving the interfacial tensions at the three phase contact line and film tension. Water droplets smaller than the critical size do not bear contact with the substrate and thus are not subjected to film tension. For such droplets, the force balance at the three phase contact line results in an unbalanced force which is responsible for the outward migration. Smaller water droplets instantaneously migrate radially outward until contacting with the substrate where film tension comes to play and droplets attain a temporary stable state. After some delay (hysteresis), due to continuous evaporation, the water droplets migrate continuously toward the edge of the sessile oil droplet. Irrespective of the initial volume of the water droplet dispensed, after the temporary stable state, all the droplets migrate at nearly the same linear velocity. A water droplet having smaller initial volume arrive at the edge of sessile oil droplet much earlier as compared to a larger water droplet. Experiments with flat oil-air interface in which there is inherent translational symmetry showed that migration of water droplets is only possible in the case of a curved oil-air interfaces in which the symmetry is lost and there exists a non-zero unbalanced force. During the stable configuration or migration of the water droplet, the thin film of oil avoids direct contact of the water droplet with PDMS substrate thus prevents possible pinning at the contact line and contamination. Finally, we demonstrated coalescence of two water droplets of sizes above the critical volume ratio at the axisymmetric location. Migration and coalescence of water droplets on a curved oil-air interface presented in this work may open up new frontiers in chemistry and biology particularly in applications such as functionalized foods, pharmaceutical formulations and drug delivery vehicles.

Supporting Information

Video S1 – migration of droplets above critical size, Video S2 – migration of droplets below critical size, Video S3 – droplet evaporation on a flat interface, Video S4 – droplet evaporation on a curved interface. Doc S5- Scaling analysis of the Energy minimization of water droplets of above and below critical size.

Author Information

Corresponding Author: Dr. Ashis Kumar Sen
Email: ashis@iitm.ac.in
Notes: The authors declare no competing for financial interest.

Acknowledgments

The authors thank SERB, DST, India (EMR/2014/001151) and IIT Madras (MEE1516843RFTPASHS) for the financial support. We also thank NCCRD, IIT Madras and Department of Applied Mechanics, IIT Madras for providing facility for surface and interfacial property measurements.

References

(1) Bormashenko, E. Surface Tension Supported Floating of Heavy Objects: Why Elongated Bodies Float Better? *J. Colloid Interface Sci.* **2016**, *463*, 8–12.
(2) Extrand, C. W.; Moon, S. I. Using the Flotation of a Single Sphere to Measure and Model Capillary Forces. *Langmuir* **2009**, *25* (11), 6239–6244.
(3) Keller, J. B. Surface Tension Force on a Partly Submerged Body. *Phys. Fluids* **1998**, *10* (11), 3009.
(4) Young, T. An Essay on the Cohesion of Fluids. *Philos. Trans. R. Soc. London* **1805**, *95* (0), 65–87.
(5) Buff, F. P.; Saltsburg, H. Curved Fluid Interfaces. II. The Generalized Neumann Formula. *J. Chem. Phys.* **2004**, *26* (1), 23.
(6) Boruvka, L.; Neumann, a. W. Generalization of the Classical Theory of Capillarity. *J. Chem. Phys.* **1977**, *66* (12), 5464.
(7) Pujado, P. R.; Scriven, L. E. Sessile Lenticular Configurations: Translationally and Rotationally Symmetric Lenses. *J. Colloid Interface Sci.* **1972**, *40* (1), 82–98.
(8) Johnson, R. E.; Sadhal, S. S. Fluid Mechanics of Compound Multiphase Drops and Bubbles. *Annu. Rev. Fluid Mech.* **1985**, *17* (1), 289–320.
(9) Weyer, F.; Ben Said, M.; Hötzer, J.; Berghoff, M.; Dreesen, L.; Nestler, B.; Vandewalle, N. Compound Droplets on Fibers. *Langmuir* **2015**, *31* (28), 7799–7805.
(10) Mahadevan, L.; Adda-Bedia, M.; Pomeau, Y. Four-Phase Merging in Sessile Compound Drops. *J. Fluid Mech.* **2002**, *451*, 411–420.
(11) Frohn, A.; Roth, N. *Dynamics of Droplets*; Springer Berlin Heidelberg, 2000.
(12) Neeson, M. J.; Tabor, R. F.; Grieser, F.; Dagastine, R. R.; Chan, D. Y. C. Compound Sessile Drops. *Soft Matter* **2012**, *8* (43), 11042–11050.
(13) Andreas, J. M. Inversion of an Interesting Three-Phase Emulsion. *J. Chem. Educ.* **1938**, *15* (11), 523.
(14) Abate, A. R.; Weitz, D. A. High-Order Multiple Emulsions Formed in Poly(dimethylsiloxane) Microfluidics. *Small* **2009**, *5* (18), 2030–2032.
(15) Bei, Z.; Jones, T. B.; Harding, D. R.; Frederick, C. A.; Paguio, R. R.; Nikroo, A.; Hund, J. F.; Acennas, O.; Thi, M.; Paguio, R. R.; et al. Electric Field Centering of Double-Emulsion Droplets Suspended in a Density Gradient. *Soft Matter* **2010**, *6* (10), 2312.
(16) Seo, M.; Paquet, C.; Nie, Z.; Xu, S.; Kumacheva, E.; McDonald, J. C.; Duffy, D. C.; Anderson, J. R.; Chiu, D. T.; Wu, H. K.; et al. Microfluidic Consecutive Flow-Focusing Droplet Generators. *Soft Matter* **2007**, *3* (8), 986.
(17) Lee, D.-H.; Goh, Y.-M.; Kim, J.-S.; Kim, H.-K.; Kang, H.-H.; Suh, K.-D.; Kim, J.-W. Effective Formation of Silicone-in-Fluorocarbon-in-Water Double Emulsions: Studies on Droplet Morphology and Stability. *J. Dispers. Sci. Technol.* **2002**, *23* (4), 491–497.
(18) P. G. de Gennes, F. Brochard-Wyatt and D. Quere. Capillarity and Wetting Phenomena – Drops, Bubbles, Pearls, Waves, Springer, New York, 2004 -.
(19) Princen, H. .; Mason, S. . Shape of a Fluid Drop at a Fluid-Liquid Interface. II. Theory for Three-Phase Systems. *J. Colloid Sci.* **1965**, *20* (3), 246–266.
(20) Langmuir, I. Oil Lenses on Water and the Nature of Monomolecular Expanded Films. *J. Chem. Phys.* **1933**, *1* (11), 756–776.
(21) Takamura, K.; Loahardjo, N.; Winoto, W.; Buckley, J.; Morrow, N. R.; Kunieda, M.; Liang, Y.; Matsuoka, T. Spreading and Retraction of Spilled Crude Oil on Sea Water.
(22) Pujado, P. .; Scriven, L. . Sessile Lenticular Configurations: Translationally and Rotationally Symmetric Lenses. *J. Colloid Interface Sci.* **1972**, *40* (1), 82–98.
(23) Zisman, W. A. The Spreading of Oils on Water Part I. Ionized Molecules Having Only One Polar Group. *J. Chem. Phys.* **1941**, *9* (7), 534–551.
(24) Miller, N. A. Investigation of the Tension Mechanisms Responsible for Lens Formation and a New Method for Measuring the Angles of Liquid Lenses. *J. Phys. Chem.* **1941**, *45* (6), 1025–1045.

(25) Nikolov, A.; Wasan, D. Oil Lenses on the Air–water Surface and the Validity of Neumann's Rule. *Adv. Colloid Interface Sci.* **2016**.

(26) Elcrat, A.; Neel, R.; Siegel, D. Equilibrium Configurations for a Floating Drop. *J. Math. Fluid Mech.* **2004**, *6*, 405–429.

(27) Burton, J. C.; Huisman, F. M.; Alison, P.; Rogerson, D.; Taborek, P. Experimental and Numerical Investigation of the Equilibrium Geometry of Liquid Lenses. *Langmuir* **2010**, *26* (19), 15316–15324.

(28) Ross, D. S. An Algorithm for Determining the Shapes of Floating Fluid Lenses. *J. Colloid Interface Sci.* **1992**, *154* (1), 66–76.

(29) Torza, S.; Mason, S. G. Three-Phase Interactions in Shear and Electrical Fields. *J. Colloid Interface Sci.* **1970**, *33* (1), 67–83.

(30) Aveyard, R.; Clint, J. H. Liquid Lenses at Fluid/fluid Interfaces. *J. Chem. Soc. Faraday Trans.* **1997**, *93* (7), 1397–1403.

(31) Aveyard, R.; Clint, J. H.; Nees, D.; Paunov, V. Size-Dependent Lens Angles for Small Oil Lenses on Water. *Colloids Surfaces A Physicochem. Eng. Asp.* **1999**.

(32) Rosenfeld, L.; Lavrenteva, O. M.; Nir, A.; Berejnov, V.; Leshanksy, A. M.; Lavrenteva, O. M.; Nir, A.; Bialik-Rosenfeld, L.; Lavrenteva, O. M.; Nir, A.; et al. On the Thermocapillary Motion of Partially Engulfed Compound Drops. *J. Fluid Mech.* **2009**, *626* (4), 263–289.

(33) Lavrenteva, O. M.; Rosenfeld, L.; Nir, A. Shape Change, Engulfment, and Breakup of Partially Engulfed Compound Drops Undergoing Thermocapillary Migration. *Phys. Rev. E* **2011**, *84* (5), 56323.

(34) Aratono, M.; Toyomasu, T.; Ikeda, N.; Takiue, T. Thermodynamics of Formation of and Adsorption at Interfaces with a Floating Lens. *J. Colloid Interface Sci.* **1999**, *218* (2), 412–422.

(35) Shao, Y.; Van de Ven, T. G. M. Spinning of Partially Engulfed Drops. *Langmuir* **1989**, *5* (5), 1234–1241.

(36) Zhang, Y.; Chatain, D.; Anna, S. L.; Garoff, S. Stability of a Compound Sessile Drop at the Axisymmetric Configuration. *J. Colloid Interface Sci.* **2016**, *462*, 88–99.

(37) Phan, C. M.; Allen, B.; Peters, L. B.; Le, T. N.; Tade, M. O. Can Water Float on Oil? *Langmuir* **2012**, *28* (10), 4609–4613.

(38) Phan, C. M. Stability of a Floating Water Droplet on an Oil Surface. *Langmuir* **2014**, *30* (3), 768–773.

(39) George, D.; Damodara, S.; Iqbal, R.; Sen, A. K. Flotation of Denser Liquid Drops on Lighter Liquids in Non-Neumann Condition: Role of Line Tension. *Langmuir* **2016**, *32* (40), 10276–10283.

(40) Chaudhury, M. K.; Chakrabarti, A.; Daniel, S. Generation of Motion of Drops with Interfacial Contact. *Langmuir*. 2015, pp 9266–9281.

(41) Biswas, S.; Pomeau, Y.; Chaudhury, M. K. A New Drop Fluidics Enabled by Magnetic Field Mediated Elasto-Capillary Transduction. *Langmuir* **2016**.

(42) Joanny, J.-F. A Model for Contact Angle Hysteresis. *J. Chem. Phys.* **1984**, *81* (1), 552.

(43) Pomeau, Y.; Vannimenus, J. Contact Angle on Heterogeneous Surfaces: Weak Heterogeneities. *J. Colloid Interface Sci.* **1985**, *104* (2), 477–488.

(44) Noblin, X.; Kofman, R.; Celestini, F. Ratchetlike Motion of a Shaken Drop. *Phys. Rev. Lett.* **2009**.

(45) Susan Daniel, Manoj K. Chaudhury, J. C. C. Fast Drop Movements Resulting from the Phase Change on a Gradient Surface. *Science (80-.).* **2001**, *291*, 633.

(46) Amirfazli, A.; Neumann, A. W. Status of the Three-Phase Line Tension. **2004**, *110*, 121–141.

(47) Lafuma, A.; Quéré, D. Slippery Pre-Suffused Surfaces. *EPL* **2011**, *96* (56001).

(48) Teletzke, G. F.; Davis, H. T.; Scriven, L. E. Wetting Hydrodynamics. *Rev. Phys. Appliquée* **1988**, *23* (6), 989–1007.

(49) Myint, P. C.; Firoozabadi, A. Thermodynamics of Flat Thin Liquid Films. *AIChE J.* **2015**, *61* (9), 3104–3115.

(50) Sjöblom, J. *Emulsions and Emulsion Stability*; Taylor & Francis, 2006.

(51) Kralchevsky, P. A.; Nagayama, K. *Particles at Fluids Interfaces and Membranes : Attachment of Colloid Particles and Proteins to Interfaces and Formation of Two-Dimensional Arrays*; Elsevier, 2001.

(52) Berteloot, G.; Pham, C.-T.; Daerr, a.; Lequeux, F.; Limat, L. Evaporation-Induced Flow near a Contact Line: Consequences on Coating and Contact Angle. *EPL (Europhysics Lett.* **2008**, *83* (1), 14003.

(53) Kovalchuk, N. M.; Trybala, A.; Starov, V. M. Evaporation of Sessile Droplets. *Curr. Opin. Colloid Interface Sci.* **2014**, *19* (4), 336–342.

(54) Eggers, J.; Pismen, L. M. Nonlocal Description of Evaporating Drops. *Phys. Fluids* **2010**, *22* (11).

(55) Deegan, R. D.; Bakajin, O.; Dupont, T. F.; Huber, G.; Nagel, S. R.; Witten, T. A. Contact Line Deposits in an Evaporating Drop. *Phys. Rev. E - Stat. Physics, Plasmas, Fluids, Relat. Interdiscip. Top.* **2000**, *62* (1 B), 756–765.

(56) Gelderblom, H.; Bloemen, O.; Snoeijer, J. H. Stokes Flow near the Contact Line of an Evaporating Drop. *J. Fluid Mech* **2017**, *709*, 69–84.

(57) Bozzano, G.; Dente, M. Coalescence between Adjacent Drops Lying on the Interface of Two Liquids. *Chem. Eng. Trans.* **2013**, *32*, 1489–1494.

(58) Boreyko, J. B.; Polizos, G.; Datskos, P. G.; Sarles, S. a.; Collier, C. P. Air-Stable Droplet Interface Bilayers on Oil-Infused Surfaces. *Proc. Natl. Acad. Sci.* **2014**, *111* (21), 7588–7593.

For Table of contents only: